Prediction of Local CHF Variation along a 10 degree Inclined Large Surface Facing Downward

Uiju Jeong [a] and Sung Joong Kim [b*]
[a]*KHNP Central Research Institute, 1312 70-gil Yuseong-daero, Yuseong-gu, Daejeon 34101, Korea*
[b]*Department of Nuclear Engineering, Hanyang University, 222 Wangsimni-ro, Seongdong-gu, Seoul 04763, Korea*
[*]*Corresponding author: sungjkim@hanyang.ac.kr*

1. Introduction

Since the early 2000s, demand for research of boiling crisis at the wall facing downward has increased due to introduction of an ex-vessel strategy for efficient mitigation of severe accident. For the strategy, the passively actuated core catcher systems were designed for retention and cooling of the corium ejected from the failed reactor pressure vessel for NPPs, such as EU-ABWR, VVER, ESPWR, and EU-APR. These systems have a common feature, which is that boiling mechanism is involved in cooling process of residual heat after a core meltdown. It should be noted that the boiling process occurs at the bottom wall which is designed to be inclined at around 10° from the horizontal plane to facilitate vapor venting. This is why we chose 10° for the inclination of the heater surface in the present study.

There is a noteworthy study by Sulatskii et al. [1], who produced the CHF data by using a large plate-type heater facing downward which is quite similar with that of the core catcher system. They proposed a semi-empirical CHF model which correlated their CHF data according to the theoretical basis. But the fact that the CHF was treated uniformly throughout the entire heater surface remains a limitation of their research.

Cheung and Haddad [2] made the first attempt to predict the spatial variation of local CHF on an exterior surface of the hemispherical vessel for IVR-ERVC strategy. But, the fact that they established the momentum balance equation by postulating bubbly flow for the flow pattern remains a limitation of their model with regard to its application to the core catcher. This is because slug flow would appear in the core catcher cooling channel.

It can be concluded that none of the CHF models is available for prediction of the variation of the local CHF along the downward-facing heater surface of large and flat geometry. The aim of the present study is to develop a pool boiling CHF model for saturated water on the downward-facing surface by adopting the CHF model of Cheung and Haddad as the base model. Then, we could estimate the thermal margin of the core catcher cooling system by comparing the model prediction and the calculated heat load along the bottom wall of the core catcher [3].

2. Theoretical Modeling

Cheung and Haddad postulated that a liquid sublayer exists underneath an elongated vapor slug on downward-facing heater. The CHF is assumed to take place when liquid supply to the sublayer becomes smaller than the depletion rate of the liquid sublayer film by boiling. The rate of liquid supply could be determined by performing the two-phase boundary layer analysis. This physical framework has been kept in the present modeling. The two-phase boundary layer (TPBL) on a 10° inclined surface and the liquid sublayer underneath an elongated vapor slug are presented in Fig. 1.

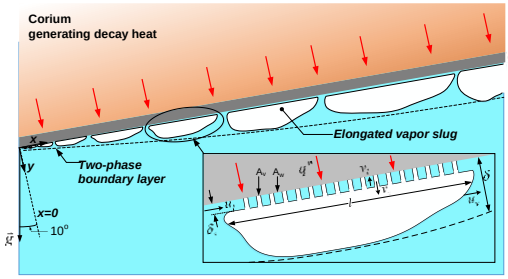

Fig. 1. Domain of the theoretical modeling.

Haramura and Katto theoretically derived correlations for thickness of the liquid film δ_s and q''_{CHF}, as expressed below:

$$(\delta_s)_{CHF} = C_1 \sigma \rho_v \left(1+\frac{\rho_v}{\rho_l}\right)\left(\frac{\rho_v}{\rho_l}\right)^{0.4}\left(\frac{h_{fg}}{q''_{CHF}}\right)^2 \quad (1)$$

$$q''_{CHF} = \rho_l h_{fg} u_l \left(\frac{A_m}{A_w}\right) = C_2 \rho_l h_{fg} u_l \frac{(\delta_s)_{CHF}}{l} \quad (2)$$

where C_1 and C_2 are the empirical constants. u_l is the local liquid velocity in the two phase boundary layer. A_m is the net flow area into the liquid film and A_w is the heater surface area occupied by the vapor slug. l is the characteristic length of the elongated vapor slug, and can be estimated by following relation, in which l is found to be approximately proportional to the boundary layer thickness δ.

$$l = C_3 \delta \quad (3)$$

where C_3 is the empirical constant having a value, which is close to 7.5. This constant was determined from the experimental observations by Kim (2016) [4]. As a result, the local CHF can be derived as follows:

$$q''_{CHF} = B \rho_v h_{fg} \left[\left(\frac{u_l \sigma}{\rho_l \delta}\right)\left(1+\frac{\rho_v}{\rho_l}\right)\left(\frac{\rho_v}{\rho_l}\right)^{-1.6}\right]^{1/3} \quad (4)$$

where B is the empirical constant determined based on C_3 and C_3 as expressed by Eq. (10).

The analysis of the TPBL starts by applying the conservation laws for mass and momentum to the boundary layer. The equations of mass conservation mass can be written in differential form:

$$\frac{d}{dx}\left[\rho_l(1-\alpha)u_l\delta\right] = \rho_l j_e - q''_{CHF}/h_{fg} \tag{5}$$

$$\frac{d}{dx}\left[\rho_v \alpha u_v \delta\right] = \rho_v j_g = q''_{CHF}/h_{fg} \tag{6}$$

where α is the local void fraction in the boundary layer. $\rho_l j_e$ is the net entrained rate of liquid mass from the ambient fluid into the TPBL by turbulent behavior, and $\rho_v j_g$ is the vapor mass flux due to vapor generation at the heater surface. The equations of conservation of momentum can be represented by one equation as follows

$$\begin{aligned}\frac{d}{dx}\left[\left\{(1-\alpha)\rho_l u_l^2 + \alpha\rho_v u_v^2\right\}\delta\right] = &-4(1-\alpha)C_f\rho_{tp}u_l^2 \\ &- C_D\alpha\rho_l(u_v-u_l)^2 - 2\rho_l j_e u_l \\ &+ 2\alpha\delta(\rho_l-\rho_v)g\cos(\theta-\pi/2)\end{aligned} \tag{7}$$

where C_f is a friction coefficient having the value of 0.005. ρ_{TP} is the density for the two-phase. C_D is the drag coefficient having a value of 2.67 according to Levy (1999). The first term in the right hand side is responsible for momentum loss due to the shear stress at the wall. The second term is responsible for the loss due to drag force, and the third term was prepared to take into account the pressure drop comes from acceleration of the entrained liquid from the outer region of the boundary layer to the velocity of liquid slug. The last term is responsible for the momentum source due to buoyancy force exerted on the vapor phase.

To solve the governing system, we need an independent equation, which is the relative velocity between the vapor and liquid phases. As in the case of Cheung and Haddad's CHF model, the following Eq. (8) for bubbly flow based on the Drift Flux Model was used with modification of the empirical constant from 1.53 to 1.94.

$$u_v = u_l + 1.94\left[\frac{\sigma g\sin\theta(\rho_l-\rho_v)}{\rho_l^2}\right]^{1/4} \tag{8}$$

The governing equations can be solved iteratively after the establishment of the adequate initial conditions, such as the TPBL thickness, local void fraction, phase velocities. As the stable formation of the two-phase boundary layer requires a specific developing length beyond 100 mm, the initial conditions were determined based on the developing length of 100 mm. It was postulated that the initial conditions are invariant along the starting region up to 100 mm.

The vapor velocity, u_{v_0}, at the initial location x_0 can be determined from a mass balance equation as following

$$\rho_v\alpha_0 u_{v_0}\delta_0 = \frac{1}{h_{fg}}\int_0^{x_0} q''_{CHF}\,dx \tag{9}$$

where, the subscript "0" in the variables means the initial value at x_0. Assuming the local CHF at the starting region to be a constant equals to $q''_{CHF,0}$, an expression for the initial value of vapor velocity can be obtained by integrating Eq. (9). The result is

$$u_{v_0} = \frac{x_0 q''_{CHF,0}}{\rho_v\alpha_0 h_{fg}\delta_0} \tag{10}$$

The initial liquid velocity is given by

$$u_{l_0} = \frac{x_0 q''_{CHF,0}}{\rho_v\alpha_0 h_{fg}\delta_0} - 1.94\left[\frac{\sigma g\sin\theta(\rho_l-\rho_v)}{\rho_l^2}\right]^{1/4} \tag{11}$$

Applying Eq. (4) at $x=x_0$ into Eq. (11), an expression can be derived implicitly as follows:

$$\left(\frac{q''_{CHF,0}}{B\rho_v h_{fg}}\right)^3 = \left[\frac{x_0 q''_{CHF,0}}{\rho_v\alpha_0 h_{fg}\delta_0} - 1.94\left(\frac{\sigma g\sin\theta(\rho_l-\rho_v)}{\rho_l^2}\right)^{1/4}\right] \times \left[\left(\frac{\sigma}{\rho_l\delta_0}\right)\left(1+\frac{\rho_v}{\rho_l}\right)\left(\frac{\rho_v}{\rho_l}\right)^{-1.6}\right] \tag{12}$$

The value of initial thickness of the TPBL δ_0 can be determined iteratively from Eq. (12) if the initial values of the void fraction and the local CHF are known.

Initial void fraction at the starting region could be determined based on the measurement from the experimental work by Jeong and Kim (2018) as 0.95 [4]. They used the optical fiber microprobe to accurately measure both the local void fraction and the bubble hovering period Δt_v. The hovering period was used in determination of the empirical constant C_1 by following Eq. (13). The empirical constant B could be determined based on Eq. (14).

$$C_1 = \frac{\Delta t_v}{\sigma\rho_v\rho_l}\left(1+\frac{\rho_v}{\rho_l}\right)^{-1}\left(\frac{\rho_v}{\rho_l}\right)^{-0.4}\left(\frac{q''_{CHF,0}}{h_{fg}}\right)^3 \tag{13}$$

$$B = (C_1/C_3)^{1/3} = 0.0464 \tag{14}$$

The hovering period was found to be 0.36 s, and the local CHF at the beginning region is 355 kW/m^2 given in the paper by Jeong et al. [5]. Once the initial conditions are determined, Eqs. (4) – (8) can be solved

simultaneously to determine the spatial variation of the local CHF along the heater surface.

It should be noted that the present CHF model is only applicable to the plate-type heater facing downward with inclination angle of 10° because the initial conditions and the empirical constant B were determined based on the CHF experiments in which only 10° inclined heater was used.

3. Results and Discussion

Over the geometric range of $0 < x < 3$ m for saturated water at 1.5 bar, the local quantities in the TPBL flow could be calculated as shown in Figs. 2 – 5. Result, shown in Fig. 2, on the local void fraction seems to agree well with the constant void fraction postulation. The consistency between the model calculation results and the experimental observation shows that the present CHF model satisfies a minimum a necessary requirement for the physically adequate model.

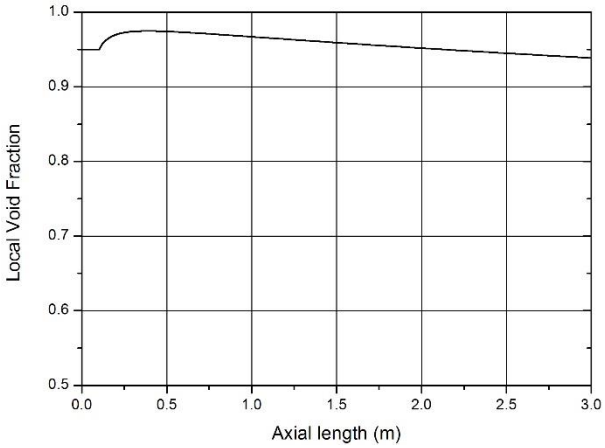

Fig. 2. Spatial variation of the local void fraction along heater surface.

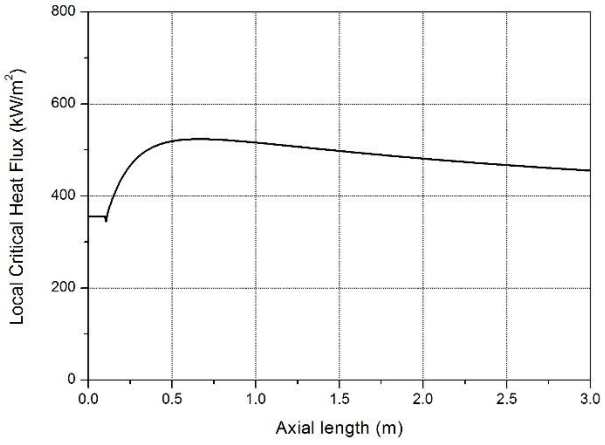

Fig. 3. Spatial variation of the local critical heat flux (CHF) along heater surface.

As seen in Fig. 3, the local CHF profile can be divided spatially into two regions. In the first region, up to 0.5 m, the local CHF rose quite rapidly and reached the maximum value. This trend can be explained by examining the rapid flow acceleration due to low flow velocity and the resultant small amounts of both shear stress and the acceleration loss by the entrained motion of ambient liquid into the TPBL region. Such rapid acceleration process could be presented well in Fig. 4. Thus, this region can be called "weak Friction and Acceleration loss region (weak F-A loss region)." In second region, $0.5 < x < 3$ m, continuous and gradual decrease of the local CHF was appeared. Such trend can be understood by considering slowing down process of acceleration behavior of the TPBL due to large amount of both the shear stress and the acceleration loss, while the TPBL thickness linearly rises along the entire heater surface, as clearly seen in Fig. 5. Thus, the second region can be called "Friction and acceleration loss dominant region (F-A loss dominant region)." The prediction on the local CHF showed that the most upstream region over the heater surface is mostly susceptible to occurrence of boiling crisis.

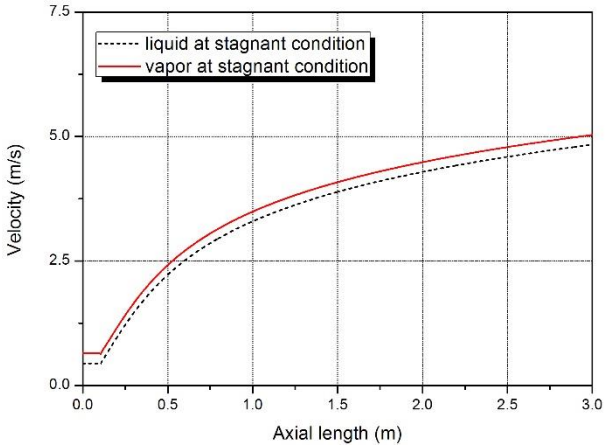

Fig. 4. Spatial variation of the liquid and vapor phase velocities.

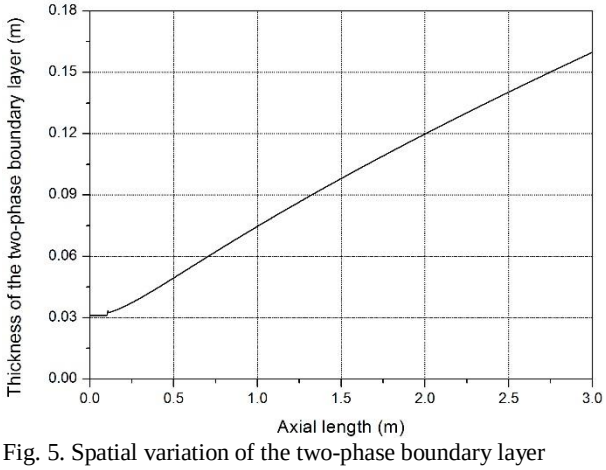

Fig. 5. Spatial variation of the two-phase boundary layer thickness.

Unfortunately, this model could not be validated because none of the previous studies was carried out to investigate the local CHF regarding its spatial distribution at the downward-facing heater of large and

flat geometry. Thus, at present, the model prediction uncertainty could not be quantified. Inevitably, instead of full validation, we roughly estimated the validity of the proposed model by employing the experimental results from Rouge (1997) [6] and Sulatskii et al. (2002). Rouge performed the CHF experiments in the facility called SULTAN, in which large-size heater was used. He proceeded the experiments by dividing the program into two campaigns. In a first campaign, the CHF data were produced by taking inlet temperature and flow rate as main variables in a vertical channel with a gap of 30 mm. Rouge observed that the boiling crisis generally occurs within the most downstream region of heater. In a second campaign, same with the core catcher for EU-APR and EU-ABWR, a 10° inclined channel from horizon was used in CHF experiment. However, Rouge didn't leave any comments about location at which the boiling crisis generally occurs. We speculated about the reason for absence of the information about location susceptible to boiling crisis that the boiling crisis occurs at somewhere in the upstream region. Interestingly, Sulatskii et al. (2002) reported valuable observations, in which the boiling crisis always take places over a length of 50 to 120 mm from the beginning of the heater regardless of its length. Their observation is definitely consistent with the calculation results from the present model.

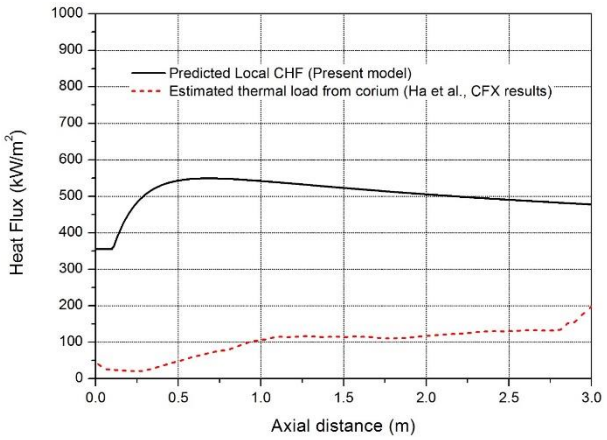

Fig. 6. Comparison between predicted local CHF profile from the present model and the estimated thermal load at bottom wall of the core catcher body.

Finally, we could utilize the developed CHF model for estimation of the thermal margin of the core catcher cooling system. The estimation could made by comparing the model prediction and the calculated thermal load along the bottom wall of the core catcher, as shown in Fig. 6. The thermal load profile was calculated by the CFX code by considering the natural circulation phenomenon of the molten corium on the core catcher body [3]. Figure 6 clearly shows that although the estimated thermal load has large uncertainty, the thermal margin is considered to be large enough.

4. Conclusions

Although this study couldn't complete validation of the present CHF model by comparing model prediction with the experimental data, it can be said that there is a unique feature regarding the spatial variation of the local CHF along the heater surface. In other words, contrary to case of vertical flow boiling, the most upstream region in heater surface facing downward may be not the safety region in regard to the boiling crisis. This means that we need to accurately predict the local heat flux level at the most upstream region of bottom wall in the core catcher system.

REFERENCES

[1] A. A. E. Sulatskii, O. D. Chernyi, and V. K. Efimov, Investigation of the crisis of heat transfer under conditions of boiling on an inclined surface facing downward, High Temp., Vol. 40, p. 912, 2002.
[2] F. B. Cheung and K. H. Haddad, A hydrodynamic critical heat flux model for saturated pool boiling on a downward facing curved heating surface, Int. J. Heat Mass Transf., Vol. 40, p. 1291, 1997.
[3] K. S. Ha, B. W. Rhee, and R. J. Park, Coolability of an ex-vessel core catcher induced by natural circulation flow, Proceedings of ICAPP, April.6-9, 2014, Sharlotte, USA.
[4] U. Jeong and S. J. Kim, Subcooling effect on boiling heat transfer of downward-facing inclined surface under low flow and pressure, Int. J. Heat Mass Transf., Vol. 127, p. 182, 2018.
[5] U. Jeong, H. H. Son, and S. J. Kim, Influence of the aligned flow obstacles on critical heat flux in two-phase boundary layer flow under a low flow condition, Int. J. Heat Mass Transf., Vol. 121, p. 1234, 2018.
[6] S. Rouge, SULTAN test facility for large-scale vessel coolability in natural convection at low pressure, Nucl. Eng. Des., Vol. 169, p. 185, 1997.